MOLECULAR ECOLOGY

Molecular Ecology (2012) **21**, 2775–2787 doi: 10.1111/j.1365-294X.2012.05572.x

Persistent genetic signatures of historic climatic events in an Antarctic octopus

J. M. STRUGNELL,* P. C.WATTS,†[1] P. J. SMITH‡ and A. L. ALLCOCK§[1]

*Department of Genetics, La Trobe Institute for Molecular Science, La Trobe University, Bundoora, 3086 Vic., Australia, †Institute of Integrative Biology, University of Liverpool, The Biosciences Building, Crown Street, Liverpool L69 7ZB, UK, ‡Museum Victoria, GPO Box 666, Melbourne, Vic. 3001, Australia, [4]Department of Zoology, Ryan Institute, National University of Ireland, Galway, Ireland

Abstract

Repeated cycles of glaciation have had major impacts on the distribution of genetic diversity of the Antarctic marine fauna. During glacial periods, ice cover limited the amount of benthic habitat on the continental shelf. Conversely, more habitat and possibly altered seaways were available during interglacials when the ice receded and the sea level was higher. We used microsatellites and partial sequences of the mitochondrial cytochrome oxidase 1 gene to examine genetic structure in the direct-developing, endemic Southern Ocean octopod *Pareledone turqueti* sampled from a broad range of areas that circumvent Antarctica. We find that, unusually for a species with poor dispersal potential, *P. turqueti* has a circumpolar distribution and is also found off the islands of South Georgia and Shag Rocks. The overriding pattern of spatial genetic structure can be explained by hydrographic (with ocean currents both facilitating and hindering gene flow) and bathymetric features. The Antarctic Peninsula region displays a complex population structure, consistent with its varied topographic and oceanographic influences. Genetic similarities between the Ross and Weddell Seas, however, are interpreted as a persistent historic genetic signature of connectivity during the hypothesized Pleistocene West Antarctic Ice Sheet collapses. A calibrated molecular clock indicates two major lineages within *P. turqueti*, a continental lineage and a sub-Antarctic lineage, that diverged in the mid-Pliocene with no subsequent gene flow. Both lineages survived subsequent major glacial cycles. Our data are indicative of potential refugia at Shag Rocks and South Georgia and also around the Antarctic continent within the Ross Sea, Weddell Sea and off Adélie Land. The mean age of mtDNA diversity within these main continental lineages coincides with Pleistocene glacial cycles.

Keywords: circumpolar distribution, glacial cycles, octopod, population structure, southern ocean

Received 24 August 2011; revised received 9 February 2012; accepted 16 February 2012

Introduction

Changes in the climatic, tectonic and glacial history of Antarctica have been integral in shaping contemporary patterns of biodiversity in the Southern Ocean marine biota (Prothero & Berggren 1992; Clarke & Crame 1992, 2003), with major episodes of radiation and speciation correlating with periods of change in the climate and/or oceanographic features (Pastene *et al.* 2007; Strugnell *et al.* 2008; Wilson *et al.* 2009). Of fundamental importance are the Pliocene–Pleistocene glacial cycles. During glacial maxima, much of the continental shelf and slope regions were covered in grounded ice (Thatje *et al.* 2005; Newman *et al.* 2009), reducing available habitat and limiting the ranges of benthic species to isolated refugia; conversely, during warmer interglacial periods, the retreating grounded ice allowed species to expand their ranges.

Biological and geological studies support the existence of refugia on the Antarctic shelf itself during

Correspondence: Jan Strugnell, Fax: +61 3 9479 2480; E-mail: j.strugnell@latrobe.edu.au

[1]These authors contributed equally to this work.

glacial periods (Newman *et al.* 2009). For example, during the last glacial maximum (LGM) (~25–19 years ago), the south-western Ross Sea, Prydz Bay and deeper parts of the Bransfield Basin (between the north-western Antarctic Peninsula and the South Shetland Islands) were likely free of grounded ice, whilst ice sheets approached the shelf break around most of Antarctica (Barnes & Hillenbrand 2010). During interglacial periods, pathways for (re-)colonization depended on species dispersal capabilities and seascape. Intriguingly, recent models indicate that the West Antarctic Ice Sheet collapsed periodically during Pleistocene interglacial periods, potentially opening a direct seaway between the Ross and Weddell Seas (Pollard & DeConto 2009). The extent to which contemporary populations retain genetic signatures of these historical events remains unclear, as large-scale intraspecific studies of Southern Ocean invertebrates are lacking because of the costs and logistical difficulties in procuring sufficient samples.

Nonetheless, for Southern Ocean taxa, there have been some intraspecific studies of limited geographic range. Typically, these emphasize the role of contemporary oceanographic features in driving patterns of divergence, particularly for pelagic organisms and benthic species with pelagic larvae. For example, weak spatial genetic structure occurs along large areas of the main Antarctic continental shelf while sub-Antarctic island populations, such as from South Georgia and the South Orkney Islands, are often genetically different (e.g. Hoffman *et al.* 2011); other work has identified a role for the Antarctic Circumpolar Current (ACC) in aiding dispersal (Thornhill *et al.* 2008; Matschiner *et al.* 2009; Raupach *et al.* 2010). The few studies that have examined spatial genetic structure in directly developing Antarctic benthic invertebrates have reported higher levels of genetic differentiation (e.g. Hoffman *et al.* 2010) as expected for species that lack a pelagic stage. Indeed, benthic species with direct development should be particularly prone to accumulating genetic differences among areas and retaining historic patterns of genetic divergence.

The benthic octopod *Pareledone turqueti* (Joubin, 1905) is an ideal model to examine effects of historic climatic events on direct-developing Antarctic benthic invertebrates. *P. turqueti* has a circumpolar distribution and also occurs around islands in the region where it inhabits depths from less than 100 m to ~1000 m. Females produce between 22 and 60 eggs that grow to 20 mm length prior to fertilization (Barratt *et al.* 2008). Planktonic hatchlings are believed to result only in octopod species with eggs <10 mm length (Boletzky 1974). The eggs of *P. turqueti* are amongst the largest reported for octopods (see comparative tables in Barratt *et al.* 2008 and data for deep-sea species in Barratt *et al.* 2007) and are believed to hatch as benthic young. A study of *P. turqueti* using allozyme electrophoresis (Allcock *et al.* 1997) showed substantial genetic divergence (F_{ST} = 0.74 between the adjacent islands of South Georgia and Shag Rocks; see Fig. 1 for locations), and thus, this species is expected to show marked spatial genetic structure across its range. Large numbers of *P. turqueti* have been collected throughout the Southern Ocean from International Polar Year/Census of Antarctic Marine Life efforts, fish surveys, and the Alfred Wegener Institute. Moreover, the broader taxonomic group to which this species belongs is well characterized and enables the use of a calibrated molecular clock (Strugnell *et al.* 2008) to identify historic events associated with periods of genetic divergence.

Here, we use nuclear (microsatellite) genetic markers to identify features that drive the distribution of genetic diversity among contemporary populations of *P. turqueti*. Samples are also characterized using mitochondrial (MT-CO1) sequence data to take advantage of a calibrated molecular clock and place periods of genetic divergence in historic context. This integrated approach provides an understanding of the relative importance of historical and contemporary processes that influence spatial genetic structure in Antarctic benthic marine invertebrates.

Methods

Specimen collection

Pareledone turqueti samples were collected from locations that circumvent the Antarctic continent (Fig. 1) using benthic trawls (Agassiz and otter trawls) between 95–1044 m in 1987–2009. A piece of tissue from each octopus was stored in 70–100% ethanol for molecular work, prior to preserving whole animals for taxonomic identification by ALA (Louise Allcock). Sampling effort was not consistent, with areas off the South Shetland Islands, South Georgia, Shag Rocks, Ross Sea and Adélie Land sampled intensively using large trawls, whereas sampling at the remaining locations was opportunistic.

Microsatellite genotyping and data analyses

Samples were genotyped at 10 of the microsatellite loci previously described for *P. turqueti* (Strugnell *et al.* 2009; and Data S1, Supporting information). Samples from Adélie Land were not available for microsatellite genotyping. PCR conditions and thermal cycling conditions are provided in Strugnell *et al.* (2009). PCR products were pooled into one of the two genotyping panels along with GENESCAN-500 LIZ size standard (Applied

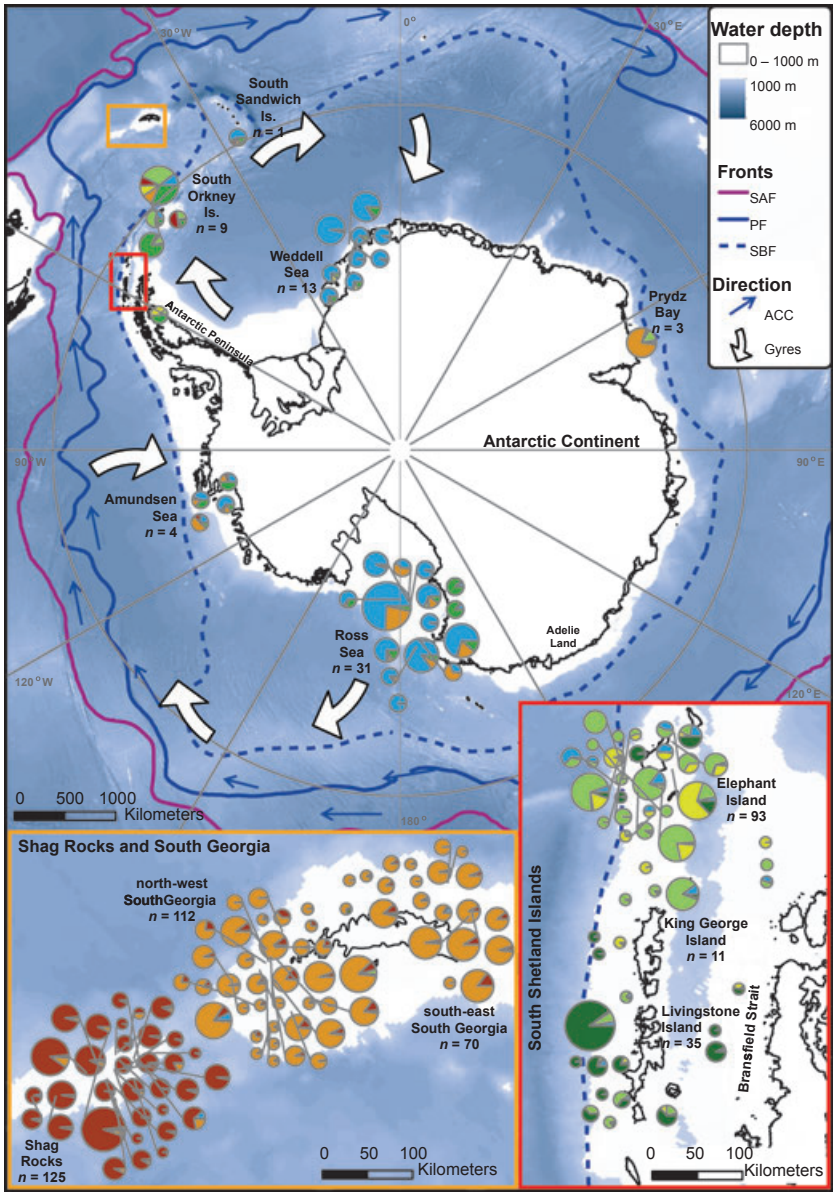

Fig. 1 Map of Antarctica indicating the sample sites and sample sizes for *Pareledone turqueti* and the main geographic regions mentioned in the text. Pie charts are proportional to sample sizes and indicate the average proportion of membership of the sample to $K = 6$ model clusters (Structure analysis of microsatellite loci). Pie charts on continental Antarctica (bottom right) are depicted 50% bigger than those in the South Shetland Islands and Shag Rocks/South Georgia panels to aid visualization. Straight lines link pie charts to the location from which the individuals were sampled. Individual membership proportions for $K = 3$ and $K = 6$ model clusters are provided in Fig. S2, Table S3 (Supporting information). Fronts of the Antarctic Circumpolar Current (ACC) are indicated: SAF, Sub-Antarctic Front; PF, Polar Front; SBF, Southern Boundary Front. The direction of the ACC is indicated with blue arrows and the flow of the Ross Sea and Weddell Sea gyres is indicated with white arrows.

Biosystems) and separated by capillary electrophoresis on an ABI3130xl (Applied Biosystems).

FSTAT v.2.9.3 (Goudet 1995) was used to calculate allelic richness (A_R) standardized to nine individuals and expected heterozygosity (H_e) for samples that contained 10 or more individuals (Table 1); at this stage, the large sample at South Georgia was divided into two groups, North-West and South-East, which represented sampling regions previously investigated (Allcock *et al.* 1997). Genetic differentiation among pairs of large samples (F_{ST}) was calculated using FSTAT, with the significance of estimates of pairwise F_{ST} from zero assessed through 2000 permutations of genotypes between populations.

Table 1 Sample sizes and summary genetic diversity statistics for samples of *Pareledone turqueti* genotyped at (i) 10 microsatellite loci and (ii) a 654-bp region of MT-CO1

		South Georgia		Antarctic Continental Shelf			South Shetland Islands		
	Shag Rocks	North West	South East	Weddell Sea	Ross Sea	Adélie Land	Living-stone	King George	Elephant
n_{mic}	125	112	70	13	31		35	11	93
H_e	0.776	0.802	0.787	0.796	0.883		0.829	0.851	0.813
N_a	29.4	30.6	25.2	10.5	19.4		19.1	9.6	33.4
A_R	8.4	9.5	9.2	9.2	11.2		9.7	9.2	10.0
n_{co1}	48	52	32	16	45	20	13	4	15
h	0.613	0.307	0.583	0.667	0.627	0.742	0.462	0.000	0.248
N_h	8	4	6	5	12	8	2	1	2
S	5	3	6	7	13	12	4	0	1
π	0.0012	0.0005	0.0012	0.0036	0.0034	0.0053	0.0031	0.0000	0.0003
A_r	3.159	1.511	2.571	3.598	4.139	4.252	1.000	-	0.990

See Fig. 1 for sample locations. Small samples from the South Orkney Islands (n = 9), South Sandwich Islands (n = 1), Prydz Bay (n = 3) and the Amundsen Sea (n = 4) are not included.
n_{mic}, sample size; H_e, expected heterozygosity; N_a, average number of alleles per locus; A_R, allelic richness; n_{co1}, sample size; h, haplotype diversity; N_h, number of haplotypes; S, number of polymorphic sites; π, nucleotide diversity; A_r, haplotype richness after rarefaction to 13 individuals – data not available for King George Island as there are insufficient samples.

To infer spatial genetic structure without predefined subdivision, we used the Bayesian model-based clustering approach implemented by Structure v.2.3.1 (Pritchard *et al.* 2000) to simultaneously identify populations (clusters) and assign individuals to these populations. Five independent runs of Structure were made for values of K from 1 up to 15 using the admixture model and correlated allele frequencies, with run lengths of 200 000 iterations after a burn-in of 20 000 iterations. The most pronounced level of population subdivision, and further subdivisions, was identified using the method of Evanno *et al.* (2005), implemented by STRUCTURE HARVESTER v.0.56.3 (http://taylor0.biology.ucla.edu/struct_harvest/).

mtDNA sequencing and data analyses

Representative samples were further characterized by sequencing part of the cytochrome oxidase c subunit 1 (MT-CO1). DNA extraction and sequencing were carried out at the barcoding facility at Guelph, Canada (details in Allcock *et al.* 2011) and at the National Institute of Water and Atmospheric Research, New Zealand. Sequence data are available on the Barcode of Life Data System [project folder 'Pareledone turqueti (PARAL)' on BOLD] and in GenBank (Accession numbers JN242814–JN243099).

ARLEQUIN v.3.5.1.2 (Excoffier *et al.* 2005) was used to calculate genetic diversity statistics; haplotype diversity (h), number of polymorphic sites (S) and nucleotide diversity (π). CONTRIB (Petit *et al.* 1998) was used to standardize for variation in sample size. A haplotype network was generated from the MT-CO1 sequence data using TCSV.1.21 (Clement *et al.* 2000), which constructs networks using maximum parsimony. The probability threshold that infers that character changes defining connections are because of a single mutation was increased from the default setting of 95–99% in one per cent increments. Missing data were designated in TCSV.1.21 as 'gaps = missing data' (rather than 'gaps = 5th state').

Both maximum likelihood (ML) and Bayesian methods were used to construct phylogenetic trees. JMODELTESTV.3.8 (Posada & Crandall 1998) was used to determine the most appropriate model of sequence evolution for phylogenetic analyses. The AIC (Akaike information criterion) favoured the GTR + G + I model for the MT-CO1 sequence data. However, the addition of a proportion of invariable sites can create a strong correlation between the proportion of invariable sites and the alpha parameter of the gamma distribution (Yang 1993; Sullivan *et al.* 1999), making it impossible to estimate both parameters reliably. Therefore, we repeated our analyses without +I; the topology was consistent between analyses. The papillated *Pareledone aequipapillae*, *Pareledone charcoti*, *Pareledone albimaculata*, *Pareledone cornuta*, *Pareledone panchroma*, *Pareledone serperastrata*, *Pareledone subtilis* and *Pareledone aurata* were used as outgroups (Strugnell *et al.* 2008). ML analysis was performed using the RAxML web-server (vital-IT Unit of the Swiss Institute of Bioinformatics) (Stamatakis 2006). Details of the Bayesian phylogenetic analyses (using BEAST v.1.5.4 Drummond & Rambaut 2007) including estimation of haplotype divergence times are provided in Data S1 (Supporting information).

Historical fluctuations in population size were detected using Fu's F_s (Fu & Li 1993), mismatch analysis (Rogers & Harpending 1992; Schneider & Excoffier 1999) and Bayesian skyline plots (Drummond *et al.* 2005) of MT-CO1 sequences. The populations examined were the distinct clusters identified by Structure (see Results; Figs S1 and S2, Supporting information); three samples, each from an isolated area (Ross Sea, Weddell Sea and Adélie Land), were examined also. Fu's F_s and the mismatch analysis were calculated using ARLEQUIN v.3.5.1.2 (Excoffier *et al.* 2005) with a randomization procedure used to test the significance of F_s, and for the mismatch analysis, a generalized least-square approach used to estimate parameters associated with sudden population expansion (Excoffier *et al.* 2005; Schneider & Excoffier 1999). The validity of a model of sudden expansion is determined from the sum of squared deviations (SSD) between observed and the expected mismatch distributions and by the raggedness index (Harpending 1994). Where a model of sudden population expansion was not rejected, an estimate of the time since expansion (t) was made from $t = \tau/(2\mu k)$, where τ = expansion time estimator, μ = mutation rate and k = sequence length (Patarnello *et al.* 2007). Ninety-five per cent CIs around expansion estimates are estimated using a parametric bootstrap (BS) procedure (Excoffier *et al.* 2005). Signatures of fluctuations in population size were also examined using Bayesian skyline plots, which were calculated using BEAST v.1.6.2 (Drummond & Rambaut 2007).

We used a HKY substitution model, empirical base frequencies and applied a strict clock rate prior. We set the sampling frequency to 3000 but varied the chain length between analyses to ensure that the estimated sample sizes were above 200. Model performance and skyline plot analysis were performed in TRACER v1.5 (Rambaut & Drummond 2003).

Results

Genetic diversity

We genotyped more than 450 samples of the benthic octopus *Pareledone turqueti* at 10 microsatellite loci (Data S1, Table S1, Supporting information) from locations that circumvent Antarctica (Fig. 1). Just nine (out of 254 tests over all samples) pairs of loci had a significant linkage disequilibrium ($P < 0.05$ after correction for multiple testing within each of the eight large sample regions – Data S1, Table S1, Supporting information). Because the majority (6) of these tests occurred within one sample (ELI) and no locus pair was out of linkage equilibrium across several populations, all loci were retained for analyses. Most sample-locus comparisons did not meet expected Hardy–Weinberg equilibrium conditions (Table S1, Supporting information), which is likely some form of Wahlund effect expected given this species' benthic existence and the broad distances covered within each sample region (see Fig. 2); thus, estimates of pairwise F_{ST} should be interpreted with caution and are provided for comparative purposes.

Genetic diversity at the 10 unlinked microsatellite loci was high, with expected heterozygosities (H_e) greater than 0.77 and allelic richness (A_R) greater than eight in all samples (Table 1). Genetic diversity was lower at Shag Rocks and South Georgia than in areas closer to the Antarctic continent, but this qualitative difference in genetic diversity between regions was not significant [$P > 0.05$ for both H_e and A_R using a permutation test (Goudet 1995)].

After removal of very short sequences, the mtDNA data set comprised 262 sequences of 654 bp length, which represented 35 different haplotypes. The mean intraspecific variation in MT-CO1 sequences was 1.03% (range 0–2.6%), with highest haplotype diversity off Adélie Land and then in the Weddell and Ross Seas, and the least diversity in samples from Elephant Island and North West South Georgia (Table 1). There were significant differences ($P = 0.039$, unpaired t-test) in MT-CO1 haplotype diversity (standardized for sample size, i.e. A_r) between the samples from Shag Rocks/South Georgia and those from continental Antarctica (Weddell Sea, Ross Sea and Adélie Land), but not between Shag Rocks/South Georgia and all other Antarctic samples ($P = 0.729$, unpaired t-test). The Ross Sea, Adélie Land and Shag Rocks samples have the most private (unique to those samples) haplotypes ($n = 7$, 4 and 4, respectively) (Fig. 2).

Spatial structure

Genetic differentiation between locations, measured using microsatellites, was moderate to low, with just seven estimates of pairwise $F_{ST} > 0.1$ (Table S2, Supporting information). The lowest value of F_{ST} (=0.001) occurred between the two areas around South Georgia (suggesting panmixia). Elsewhere, significant ($P < 0.05$) values of pairwise F_{ST} generally were observed, with the following patterns prominent: (i) large differences between South Georgia and Shag Rocks; (ii) greatest genetic differentiation between South Georgia/Shag Rocks and all other locations (except for the Shag Rocks-King George Island comparison); and (iii) levels of genetic differentiation between locations outside South Georgia/Shag Rocks significant only half the time (Table S2, Supporting information). The level of genetic differentiation between samples did not depend upon the geographic distance separating them ($r = 0.14$,

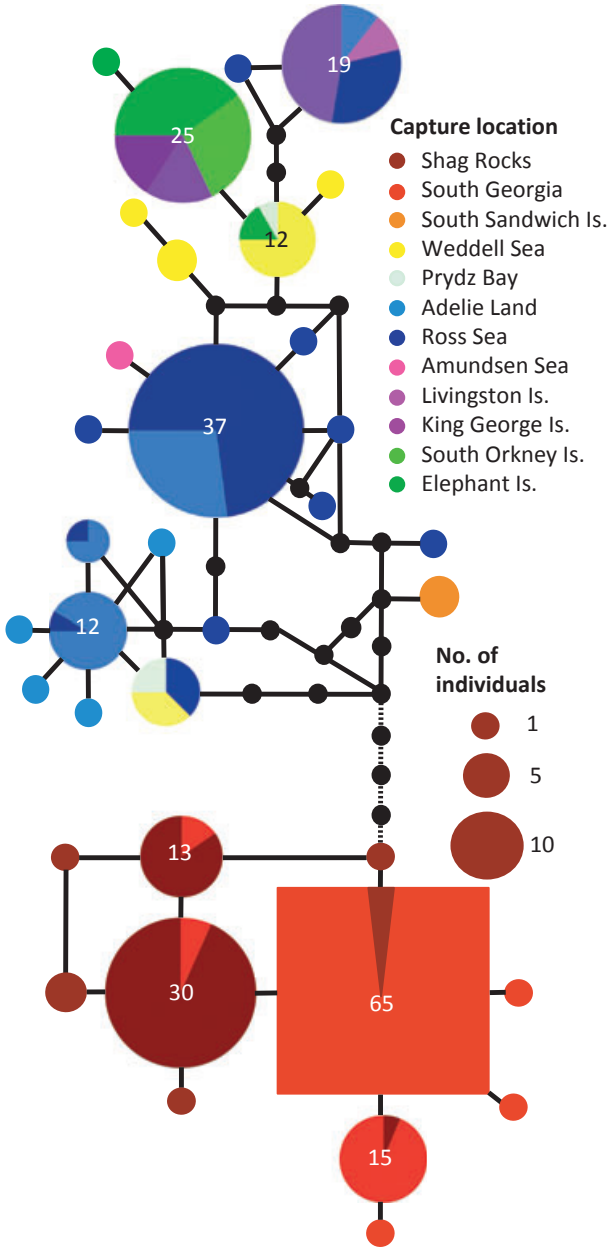

Fig. 2 Haplotype network based on *Pareledone turqueti* MT-CO1 sequence data (95% probability threshold). The haplotype with the highest outgroup probability is displayed as a square, while other haplotypes are displayed as circles. The size of circles/square indicates number of specimens, with abundances >10 provided; colours represent capture locations, and small black circles indicate absent haplotypes. Dashed lines indicated network connections that break under a 98% probability threshold.

$P = 0.30$, Mantel test) (Data S1, Fig. S3, Supporting information).

Structure analysis identified three distinct clusters (Figs S1 and S2, Table S3, Supporting information) that correspond to the locations of (1) Shag Rocks (average proportion of membership of individuals to cluster 1, $Q_1 = 0.93$), (2) South Georgia and Prydz Bay ($Q_2 > 0.85$), (3) all other Southern Ocean samples ($Q_3 = 0.64$–0.99) (Figs S1 and S2, Supporting information), reflecting the patterns of pairwise differences described above apart from the placement of the small ($n = 3$) Prydz Bay sample. Beneath the most pronounced partition of the data set was a further subdivision of cluster (3) above (Fig. 1, Figs S1 and S2, Table S3, Supporting information) into four model clusters that correspond to: (3) Weddell Sea and Ross Sea ($Q_{3*} = 0.86$ and 0.71) and to a lesser extent the South Sandwich Islands ($n = 1$; $Q_{3*} = 0.56$) and Amundsen Sea ($Q_{3*} = 0.38$); (4) King George ($Q_{4*} = 0.59$) and Livingstone Islands ($Q_{4*} = 0.77$) and to a lesser extent the South Orkney Islands ($n = 4$; $Q_{4*} = 0.40$); and (5) Elephant Island ($Q_{5*} = 0.57$). The final cluster (6) was geographically undefined, but had greatest association with samples from Elephant Island ($Q_{6*} = 0.23$) and King George Island ($Q_{6*} = 0.12$) (Fig. 1, Fig. S2, Table S3, Supporting information). Thus, the overriding pattern of genetic structure is divergence between Shag Rocks and South Georgia, as well as between these islands and all other Southern Ocean locations; some distant locations on the Antarctic continental shelf are weakly differentiated, most notably the samples from the Ross Sea and Weddell Sea (Fig. 1, Fig. S2, Table S3, Supporting information).

A single MT-CO1 haplotype network was constructed under a 95% probability threshold (Fig. 2). An identical haplotype network was constructed under a 96% and 97% probability threshold. The network broke into two networks under a 98% probability threshold separating South Georgia and Shag Rocks from the remaining locations. Under a 99% probability threshold, the South Sandwich Island haplotype split off and constituted a third network. Concordant with the three-cluster model, there is a deep genetic divergence (separated by at least six mutational steps) between Shag Rocks/South Georgia and all remaining locations. Broad differences exist between South Georgia and Shag Rocks, but the largest haplotypes from each of these locations also contain a small proportion of individuals from the other location.

The resulting phylogeny (Fig. 3) supports a distinct clade comprising haplotypes only found from South Georgia and Shag Rocks [posterior probability (PP) = 1.00, BS = 98]; the haplotype from the single specimen from South Sandwich Island is sister lineage to this clade (PP = 0.78, BS = 88). A second clade (clade 2: PP = 0.76, BS = 57) of all other haplotypes represents individuals from all other locations. Clade 2 may be divided into four lineages (i–iv) that are not

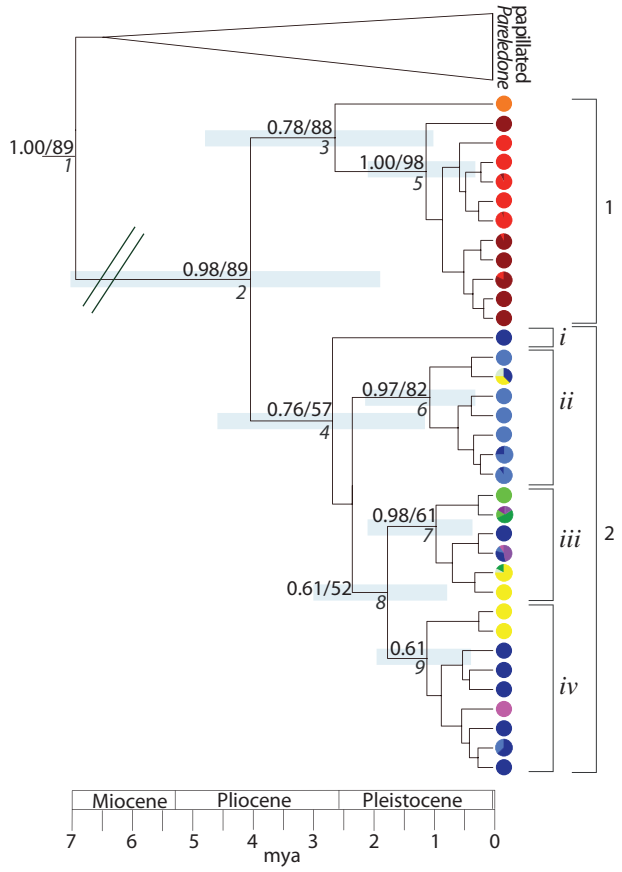

Fig. 3 Phylogenetic relationships among *Pareledone turqueti* MT-CO1 haplotypes. Bayesian phylogenetic tree based on a relaxed phylogenetic analysis (uncorrelated log-normal model) utilizing MT-CO1 of all unique *P. turqueti* haplotypes and eight 'papillated' *Pareledone* species. Colours represent capture locations (see Fig. 2). Nodes of major lineages on the tree are labelled with posterior probabilities and bootstrap values separated by a backslash. The divergence times correspond to the mean posterior estimate of their age in millions of years with 95% highest posterior density intervals around the mean; these are indicated as light blue bars in the figure (1 = 4.4–16.3, 2 = 1.9–7.1, 3 = 1.0–4.8, 4 = 1.2–4.6, 5 = 0.4–2.1, 6 = 0.3–2.1, 7 = 0.3–1.8, 8 = 0.7–3.0 and 9 = 0.4–1.9).

geographically well defined; Ross Sea individuals contribute to all four lineages. Some haplotypes are found in locations separated by large distances. For example, one haplotype is found in Adélie Land, Livingstone Island and the Amundsen and Ross Seas, while another was found in Livingstone, King George, Elephant and the South Orkney Islands; both haplotypes occur on the periphery of the haplotype network (Fig. 2).

Demography

Populations from off Shag Rocks and South Georgia probably underwent a historical population expansion – samples exhibit significantly negative values of F_s and nonsignificant SSD and indices of raggedness (Table 2) and have unimodal mismatch distributions (Fig. S4, Supporting information). Demographic expansions (using τ) suggest that *P. turqueti* underwent rapid demographic expansions during the mid-Pleistocene, at approximately 183 years ago (102–280 years ago 95% CI) in Shag Rocks and 110 years ago (48–167 years ago 95% CI) in South Georgia. Bayesian skyline plots also suggest a period of population expansion over a similar time frame in these locations (Fig. S5, Supporting information).

Although the Bayesian skyline plot (Fig. S5, Supporting information) for all remaining sample locations (not including Shag Rocks and South Georgia) indicates population expansion over a similar time frame, the samples do not exhibit significantly negative values of F_s and significant SSD and indices of raggedness (Table 2, Fig. S4, Supporting information).

A grouping of the Ross Sea, Weddell Sea, South Sandwich Island and Amundsen Sea (cluster 3* under the 6-cluster scenario) provides some apparent support for a historical population expansion on the main Antarctic shelf, but the analyses of individual samples within this group did not provide congruent evidence of a demographic expansion across all measures. The demographic signature for the Ross Sea and Weddell Sea is ambiguous, with nonsignificant values of F_s and multimodal mismatch distributions (Fig. S4, Supporting information), but the model of sudden population expansion was not rejected (Table 2). The Bayesian skyline plot for these samples shows limited population expansion in the Ross Sea, whilst no population expansion is evident in the Weddell Sea sample (Fig. S5, Supporting information).

Samples from off Adélie Land show a pattern typical of stable population structure with nonsignificant values of F_s and a significant SSD and index of raggedness (Table 2), but the corresponding Bayesian skyline plot indicates some population expansion in this sample (Fig. S5, Supporting information).

Samples from off King George and Livingstone Islands show a pattern typical of stable population structure (Table 2, Fig. S4, Supporting information), whereas the demographic signature for Elephant Island was more ambiguous, with nonsignificant F_s and a flat Bayesian skyline plot (Fig. S5, Supporting information), but the model of sudden population expansion was not rejected (Table 2).

Estimates of τ for samples other than Shag Rocks and South Georgia are provided, but not interpreted as the general evidence for population expansions is weak and the values of τ themselves have wide 95% CIs (and cannot be associated with any period) (Table 2).

Table 2. Statistical tests and associated probabilities for signatures of population expansion for $K = 3$ or six clusters of *Pareledone turqueti* identified by Structure analysis (see Results)

Structure model cluster									
$k = 3$	$k = 6$		F_s	P_{Fs}	SSD	P_{SSD}	Rag	P_{Rag}	τ (95% CI)
(1)	(1)	Shag Rocks	−4.06	0.011	0.009	0.162	0.112	0.113	0.912 (0.510–1.393)
(2)	(2)	South Georgia plus Prydz Bay	−3.81	0.013	0.001	0.596	0.130	0.480	0.547 (0.238–0.832)
(3)		All other locations	−2.75	0.180	0.058	0.010	0.156	0.002	-
	(5)	Elephant Island	0.13	0.279	0.281	0.127	0.316	0.225	2.930 (0.000–87.930)
	(4)	King George Is, Livingstone Is. plus South Orkney Is.	5.26	0.981	0.310	0.041	0.782	0.007	-
	(3)	Weddell Sea, Ross Sea, South Sandwich Is. plus Amundsen Sea	−9.21	0.001	0.023	0.262	0.066	0.285	3.852 (0.881–6.539)
		Ross Sea	−2.22	0.147	0.039	0.402	0.098	0.529	4.900 (0.328–90.873)
		Adélie Land	1.06	0.732	0.112	0.048	0.295	0.023	-
		Weddell Sea	0.59	0.639	0.045	0.361	0.151	0.332	5.500 (0.309–91.457)

Significant ($P < 0.05$) values are highlighted bold.
n, sample size; F_s, Fu's statistic; SSD, sum of square deviations to test validity of a model of sudden population expansion; Rag, raggedness index; τ, parameter to estimate timing of population expansion; 95% CI, 95% confidence interval for τ.

Timing of population divergence

Given a mutation rate of MT-CO1 for octopods (Data S1; Strugnell *et al.* 2008) of 3.81 substitutions per site per billion years (with 95% highest posterior density around this mean of 2.43–5.24), the split between clades 1 and 2 occurred ~4 Ma, during the Pliocene. The four lineages within clade 2 diverged during the transition between Pliocene and Pleistocene between 1.75 and 2.5 Ma (Fig. 3). Further divergence, particularly in the last 1250 ky, has given rise to the 35 lineages in our data set. Given that the molecular rate was calculated for all octopods, these date estimates probably reflect the lower limit of divergence because rates measured on geological timescales are slower than those measured on genealogical timescales (Ho & Larson 2006).

Discussion

Genetic analyses of the benthic octopus *Pareledone turqueti* were used to quantify genetic boundaries in the Southern Ocean and to identify historic patterns of divergence and population demography. The key findings are that (i) *P. turqueti*, a putative poor disperser, has a circumpolar distribution, (ii) samples are partitioned into distinct genetic clusters that emphasize the role of bathymetry and ocean currents in shaping gene flow, (iii) similarities between the Ross Sea and Weddell Sea populations point towards historical connectivity, (iv) a calibrated molecular clock suggests that major periods of divergence occurred in the Pliocene and Pleistocene, (v) we found support for Adélie Land, Ross and Weddell Sea refugia and (vi) recent demographic expansion around South Georgia and Shag Rocks suggests that these areas were severely impacted at glacial maxima.

Circumpolar distribution

Pareledone turqueti's circum-Antarctic distribution is unusual for a species lacking a dispersive life history stage. Adult benthic octopods swim only as an escape response and adult movement is therefore limited; adult movement is also confined to the species' bathymetric limits, which in *P. turqueti* coincide with the Antarctic continental shelf (0–1000 m). Cryptic species have been identified in many benthic Southern Ocean taxa with poor dispersal capabilities (e.g. Wilson *et al.* 2009; Krabbe *et al.* 2010; Baird *et al.* 2011), but the variation in MT-CO1 among our samples (mean K2P = 1%, range 0–2.6%) is within the reported levels of intraspecific variation in other *Pareledone* species (Allcock *et al.* 2011). Therefore, to achieve and maintain its present extensive distribution, *P. turqueti* must be capable of some long-distance dispersal. Benthic shallow-water species that lack pelagic larvae may occasionally disperse passively by rafting on floating substrata such as kelp (Leese *et al.* 2010; Nikula *et al.* 2010). Alternatively, their egg masses may be dispersed in currents either because they are laid on drifting/rafting organisms or because they become dislodged from their benthic attachment (Wilson *et al.* 2009).

Bathymetric and oceanographic drivers of population structure

Major genetic boundaries coincide with shelf habitat separated by water deeper than 1000 m. Surprisingly, microsatellite data revealed samples from South Georgia and

Prydz Bay (albeit a small sample) are more similar than samples from South Georgia and Shag Rocks (Fig. 1), even though the continental shelves of these two island groups are separated by less than 30 km. A barrier to dispersal between Shag Rocks and South Georgia has been noted for a range of taxa (Allcock *et al.* 1997; Shaw *et al.* 2004; Kuhn & Gaffney 2006), likely due to the deep water channel and the northward flow of the ACC between South Georgia and Shag Rocks. Although detouring northward after passing South Georgia, the ACC subsequently meanders southwards to pass close to Prydz Bay (Fig. 1). Sokolov & Rintoul (2007) estimated that the Southern Boundary of the ACC continues close to the continent to nearly 150°E. This southern position of the ACC during warmer periods could allow dispersal of dislodged/rafting eggs along the east Antarctic continental shelf and explain the genetic similarity of South Georgia and Prydz Bay.

The oceanographic features that limit gene flow between the South Shetland Islands and South Georgia/Shag Rocks are difficult to interpret, because there is evidence from drifter buoys that the ACC connects the Antarctic Peninsula with South Georgia/Shag Rocks (Matschiner *et al.* 2009). The large areas of shelf surrounding the South Shetland Islands would permit some gene flow between King George and Livingstone Islands to the west and Elephant Island to the east, but microsatellite data suggest there is not a single, continuous population around these islands (Fig. 1). Contradictory patterns of genetic structure in benthic marine invertebrates have been uncovered in this region, with evidence for both differentiation (Hunter & Halanych 2010) and homogeneity (Hunter & Halanych 2008). In *P. turqueti*, the pattern of spatial genetic structure around the South Shetland Islands contrasts with genetic homogeneity around South Georgia, although both regions encompass similar-sized areas of shelf. This difference highlights locality-specific influences of seascape and population history. Oceanographic features that consistently affect dispersal off the Antarctic Peninsula region have yet to be identified, largely because of the area's complex topography and the fact that it receives several different water masses, including water originating from both the ACC and Weddell Sea via the Weddell Sea gyre. The Weddell Sea gyre may also explain similarities between the Weddell Sea and the South Sandwich Islands, while it is likely that the Ross Sea gyre provides connectivity between the Ross and Amundsen Seas.

Support for a Ross Sea-Weddell Sea gateway

Similarities in genotypic composition of individuals between the widely separated (some 10 000 km apart) Ross Sea and Weddell Sea are unlikely to have resulted from inadequate sampling given the differentiation identified within the South Shetland and South Orkney Islands. The dissimilarity between the Ross and Weddell Sea populations and the (small) sample from Prydz Bay suggests that connectivity between these seas is not achieved via the ACC. One possible explanation for a lack of divergence lies in the periodic collapses of the West Antarctic Ice Sheet during the Pleistocene, which may have opened a seaway between the Ross and Weddell Seas (Scherer *et al.* 1998; Pollard & DeConto 2009). Faunal similarities between the two areas have been noted (Linse *et al.* 2006; Barnes & Hillenbrand 2010), and Linse *et al.* (2007) showed genetic similarities between the two areas, but in the absence of samples from east Antarctica, they could not reject the occurrence of dispersal via the East Wind Drift. Our microsatellite data provide greater evidence for connectivity through a seaway during ice-sheet collapses. While MT-CO1 haplotypes from the Ross Sea and Weddell Sea occur in close proximity in the haplotype network (Fig. 2), just one haplotype is shared between these regions. This difference between genetic markers may reflect the smaller mitochondrial effective population size that renders mitochondrial markers more susceptible to drift (Wilson *et al.* 1985; Moore 1995). The shared haplotype was also sampled from Prydz Bay indicating a haplotype with a circum-Antarctic distribution. Future studies should prioritize sampling in the East Antarctic to strengthen or refute evidence for the Ross Sea-Weddell Sea gateway or alternatively identify mechanisms of long-distance dispersal.

Genetic signals indicative of glacial cycles

Major divergence of MT-CO1 haplotypes was estimated to have occurred during the Pliocene producing two distinct lineages (Fig. 3): (i) animals from the Antarctic continental shelf (or close to it in the case of the South Orkney Islands) and (ii) individuals from peripheral islands of South Georgia/Shag Rocks (and also the South Sandwich Islands). Both of these lineages of *P. turqueti* survived the extreme conditions associated with Pliocene and Pleistocene glacial maxima. The absence of the distinct Shag Rocks/South Georgia mtDNA lineage in the continental populations (and *vice versa*) suggests that throughout the late Pliocene and Pleistocene glacial cycles, there was no exchange of migrants between these sub-Antarctic islands and the continental shelf.

From about 1250 ky, the start of the Mid-Pleistocene Transition, there has been a notable diversification of MT-CO1 haplotypes (Fig. 3), and this coincides with a period when there were large changes in ice volume

and sea level (Pollard & DeConto 2009). Rogers (2007) identifies 1 Ma as the start of a time of dynamic population expansion and contraction into refugia by Antarctic fauna. Such repeated glacial/interglacial cycles appear to have driven diversification and speciation in a number of benthic Antarctic taxa (e.g. Wilson *et al.* 2009), a process termed 'the Antarctic diversity pump' (Clarke & Crame 1989; Clarke & Crame 1992). It has been hypothesized that populations persisted in deep-sea refugia or glacial refugia on the shelf during glacial maxima (Thatje *et al.* 2005), although the locations of these refugia are largely undefined. Given the bathymetric distribution of *P. turqueti*, deep-sea refugia do not appear to be viable for this species, and therefore, the continental shelf lineage of *P. turqueti* is more likely to have survived glacial maxima in refugia on the shelf itself. The central position of *P. turqueti* individuals collected from Adélie Land and the Ross Sea (and to a lesser extent the Weddell Sea) in the haplotype network provides support for Pleistocene refugia in these areas, as do the high levels of allelic richness in these regions; in particular, the 'basal' position of Ross Sea haplotypes (Fig. 3) and the high number of private alleles are supportive of one or more refugia in this area. The south-western Ross Sea has been suggested as a possible ice-free area, and therefore a potential refugium, during the LGM (Barnes & Hillenbrand 2010). This presents a contrast to the effect of extensive sea ice and ice scour in extirpating southern bull kelp *Durvillaea antarctica* from the sub-Antarctic during the LGM (Fraser *et al.* 2009).

Genetic signatures of expanding populations have been reported for a range of Antarctic taxa (Pastene *et al.* 2007; Matschiner *et al.* 2009; Wilson *et al.* 2009; Raupach *et al.* 2010). The genetic signal of demographic expansion was clear around South Georgia and Shag Rocks, while there was no such evidence for demographic expansions on the main Antarctic continent. Demographic expansion at South Georgia/Shag Rocks is likely to have followed population bottlenecks caused by climatic extremes and reduced habitat during glacial maxima. It is not possible to provide a detailed interpretation of this expansion however, as the relative severity of the various glacial maxima throughout the Pleistocene is not well understood and there are also significant confidence intervals associated with our estimated dates of demographic expansion. Climate reconstructions and analyses of seafloor geomorphology do indicate however that the extent of ice sheets and glaciation at South Georgia may have been underestimated (Gersonde *et al.* 2005; Graham *et al.* 2008; Allen *et al.* 2011).

The apparent demographic rebound at Shag Rocks/South Georgia may have been influenced by an initial larger carrying capacity for *P. turqueti* in the sub-Antarctic islands because of a relative lack of competition with other octopuses. Papillated *Pareledone* species, which are diverse and abundant elsewhere in the Antarctic and sympatric with *P. turqueti* throughout their range, are not found at South Georgia or Shag Rocks. Ultimately, the combination of greater loss of habitat and concomitant genetic erosion around continental Antarctica, and relatively stable, even expanding, populations in South Georgia/Shag Rocks may account for the relatively minor differences in genetic diversity between these two areas, even though smaller and isolated populations at species' range margins are expected to have low genetic diversity. Moreover, population expansion, perhaps combined with founder effects, could account for the lack of spatial genetic structure in South Georgia and the relatively low MT-CO1 diversity in this region.

Summary

We have shown that a complex genetic population structure in a benthic octopod can be explained through a combination of bathymetric constraints and contemporary and historical processes, including potentially dispersal through a Ross Sea–Weddell Sea seaway during periods of West Antarctic Ice Sheet collapse. Furthermore, populations have persisted during Pleistocene glacial maxima, and there is evidence for refugia being located in the Ross Sea, Adélie Land, Weddell Sea and the islands of South Georgia and/or Shag Rocks.

Acknowledgements

We thank the Alfred Wegner Institute, British Antarctic Survey, Australian Antarctic Division, the South Georgia Government and MRAG for provision of sea time and to all colleagues who facilitated sea time or assisted on board. We thank the Barcode of Life Database team, particularly D. Steinke for providing MT-CO1 sequences. JMS was supported by NERC AFI NE/C506321/1 awarded to ALA and a Lloyd's Tercentenary Fellowship. This work was also funded by a CoSyst grant awarded to JMS and PCW and an Antarctic Science Bursary, a Systematics Association grant, the Edith Mary Pratt Musgrave Fund and an Australia and Pacific Science Foundation grant awarded to JMS. PJS was supported by the New Zealand Government under the NZ International Polar Year-Census of Antarctic Marine Life Project (CAML) and gratefully acknowledges the Ministry of Fisheries Science Team and Ocean Survey 20/20 CAML Advisory Group (Land Information New Zealand, Ministry of Fisheries, Antarctica New Zealand, Ministry of Foreign Affairs and Trade, and National Institute of Water and Atmospheric Research Ltd.). The manuscript was substantially improved by the constructive input of five referees. This is CAML publication no. 77 and is a contribution to Evolution and Biodiversity in the Antarctic (EBA).

Authorship

JMS and PS performed the research, JMS and PCW analysed the data, JMS, PCW and ALA designed the research and wrote the paper.

References

Allcock AL, Brierley AS, Thorpe JP *et al*. (1997) Restricted gene flow and evolutionary divergence between geographically separated populations of the Antarctic octopus *Pareledone turqueti*. *Marine Biology*, **129**, 97–102.

Allcock AL, Barratt I, Eléaume M *et al*. (2011) Cryptic speciation and the circumpolarity debate: a case study on endemic Southern Ocean octopuses using the coxI barcode of life. *Deep Sea Research Part II: Topical Studies in Oceanography*, **58**, 242–249.

Allen CS, Pike J, Pudsey CJ (2011) Last glacial–interglacial sea-ice cover in the SW Atlantic and its potential role in global deglaciation. *Quaternary Science Reviews*, **30**, 2446–2458.

Baird HP, Miller KJ, Stark JS (2011) Evidence of hidden biodiversity, ongoing speciation and diverse patterns of genetic structure in giant Antarctic amphipods. *Molecular Ecology*, **20**, 3439–3454.

Barnes DKA, Hillenbrand C-D (2010) Faunal evidence for a later quaternary trans-Antarctic seaway. *Global Change Biology*, **16**, 3297–3303.

Barratt IM, Johnson MP, Allcock AL (2007) Fecundity and reproductive strategies in deep-sea incirrate octopuses. *Marine Biology*, **150**, 387–398.

Barratt IM, Johnson MP, Allcock AL (2008) Female reproductive biology of two sympatric incirrate octopod species, *Adelieledone polymorpha* (Robson 1930) and *Pareledone turqueti* (Joubin 1905) (Cephalopoda: Octopodidae), from South Georgia. *Polar Biology*, **31**, 583–594.

Boletzky SV (1974) The larvae of cephalopoda: a review. *Thalassia Jugoslavica*, **10**, 45–76.

Clarke A, Crame JA (1989) The origin of the southern ocean marine fauna. In: *Origins and evolution of the Antarctic biota* (ed. Crame JA), pp. 253–268. The Geological Society, London.

Clarke A, Crame JA (1992) Evolution of Antarctic benthos. *Philosophical Transactions of the Royal Society of London. Series B, Biological Sciences*, **338**, 299–309.

Clarke A, Crame JA (2003) Importance of historical processes in global patterns of diversity. In: *Macroecology: Concepts and Consequences* (eds Blackburn TM and Gaston KJ), pp. 130–151. Blackwell, Malden MA.

Clement M, Posada D, Crandall KA (2000) TCS: a computer program to estimate gene genealogies. *Molecular Ecology*, **9**, 1657–1659.

Drummond AJ, Rambaut A (2007) BEAST: Bayesian evolutionary analysis by sampling trees. *BMC Evolutionary Biology*, **7**, 214.

Drummond AJ, Rambaut A, Shapiro B, Pybus OG (2005) Bayesian coalescent inference of past population dynamics from molecular sequences. *Molecular Biology and Evolution*, **22**, 1185–1192.

Evanno GS, Regnaut S, Goudet J (2005) Detecting the number of clusters of individuals using the software STRUCTURE: a simulation study. *Molecular Ecology*, **14**, 2611–2620.

Excoffier L, Laval G, Schneider S (2005) Arlequin ver. 3.0: an integrated software package for population genetics data analysis. *Evolutionary Bioinformatics Online*, **1**, 47–50.

Fraser CI, Nikula R, Spencer HG *et al*. (2009) Kelp genes reveal effects of subantarctic sea ice during the last glacial maximum. *Proceedings of the National Academy of Sciences of the United States of America*, **106**, 3249–3253.

Fu YX, Li WH (1993) Statistical tests of neutrality of mutations. *Genetics*, **133**, 693–709.

Gersonde R, Crosta X, Abelmann A *et al*. (2005) Sea-surface temperature and sea ice distribution of the Southern Ocean at the EPILOG last Glacial maximum – a circum-Antarctic view based on siliceous microfossil records. *Quaternary Science Reviews*, **24**, 869–896.

Goudet J (1995) FSTAT (vers.1.2): a computer program to calculate F-statistics. *Journal of Heredity*, **86**, 485–486.

Graham AGC, Fretwell RD, Larter DA *et al*. (2008) A new bathymetric compilation highlighting extensive paleo–ice sheet drainage on the continental shelf, South Georgia, sub-Antarctica. *Geochemistry Geophysics Geosystems*, **9**, Q07011.

Harpending HC (1994) Signature of ancient population growth in a low-resolution mitochondrial DNA mismatch distribution. *Human Biology*, **66**, 591–600.

Ho SYW, Larson G (2006) Molecular clocks: when times are a-changin'. *Trends in Genetics*, **22**, 79–83.

Hoffman JI, Clarke A, Linse K *et al*. (2010) Effects of brooding and broadcasting reproductive modes on the population genetic structure of two Antarctic gastropod molluscs. *Marine Biology*, **158**, 287–296.

Hoffman JI, Clarke AC, Linse K *et al*. (2011) Strong population genetic structure in a broadcast-spawning Antarctic marine invertebrate. *Journal of Heredity*, doi: 10.1093/jhered/esq094.

Hunter RL, Halanych KM (2008) Evaluating connectivity in the brooding brittle star *Astrotoma agassizii* across the Drake Passage in the Southern Ocean. *Journal of Heredity*, **99**, 137–148.

Hunter RL, Halanych KM (2010) Phylogeography of the Antarctic planktotrophic brittle star *Ophionotus victoriae* reveals genetic structure inconsistent with early life history. *Marine Biology*, **157**, 1693–1704.

Krabbe K, Leese F, Mayer C *et al*. (2010) Cryptic mitochondrial lineages in the widespread pycnogonid *Colossendeis megalonyx* Hoek, 1881 from Antarctic and Subantarctic waters. *Polar Biology*, **33**, 281–292.

Kuhn KL, Gaffney PM (2006) Preliminary assessment of population structure in the mackerel icefish (*Champsocephalus gunnari*). *Polar Biology*, **29**, 927–935.

Leese F, Agrawal S, Held C (2010) Long-distance island hopping without dispersal stages: transportation across major zoogeographic barriers in a Southern Ocean isopod. *Naturwissenschaften*, **97**, 583–594.

Linse K, Griffiths HJ, Barnes DKA *et al*. (2006) Biodiversity and biogeography of Antarctic and sub-Antarctic Mollusca. *Deep-Sea Research II*, **53**, 985–1008.

Linse K, Cope T, Lörz A-N *et al*. (2007) Is the Scotia Sea a centre of Antarctic marine diversification? Some evidence of cryptic speciation in the circum-Antarctic bivalve *Lissarca notorcadensis* (Arcoidea: Philobryidae). *Polar Biology*, **30**, 1059–1068.

Matschiner M, Hanel R, Salzburger W (2009) Gene flow by larval dispersal in the Antarctic notothenioid fish *Gobionotothen gibberifrons*. *Molecular Ecology*, **18**, 2574–2587.

Moore WS (1995) Inferring phylogenies from mtDNA variation: mitochondrial-gene trees versus nuclear-genetrees. *Evolution*, **49**, 718–726.

Newman L, Convey P, Gibson JAE *et al.* (2009) Antarctic paleobiology: glacial refugia and constraints on past ice-sheet reconstructions. *PAGES News*, **17**, 22–24.

Nikula R, Fraser CI, Spencer HG *et al.* (2010) Circumpolar dispersal by rafting in two subantarctic kelp-dwelling crustaceans. *Marine Ecology Progress Series*, **405**, 221–230.

Pastene LA, Goto M, Kanda N *et al.* (2007) Radiation and speciation of pelagic organisms during periods of global warming: the case of the common minke whale, *Balaenoptera acutorostrata*. *Molecular Ecology*, **16**, 1481–1495.

Patarnello T, Volckaert FAMJ, Castilho R (2007) Pillars of Hercules: is the Atlantic Mediterranean transition a phylogeographical break? *Molecular Ecology*, **16**, 4426–4444.

Petit RJ, El Mousadik A, Pons O (1998) Identifying populations for conservation on the basis of genetic markers. *Conservation Biology*, **12**, 844–855.

Pollard D, DeConto RM (2009) Modelling West Antarctic ice sheet growth and collapse through the past five million years. *Nature*, **458**, 329–333.

Posada D, Crandall KA (1998) Modeltest: testing the model of DNA substitution. *Bioinformatics*, **14**, 817–818.

Pritchard JK, Stephens M, Donnelly P (2000) Inference of population structure using multilocus genotype data. *Genetics*, **155**, 945–959.

Prothero DR, Berggren WA (1992) *Eocene Oligocene Climatic and Biotic Evolution*, pp. 569. Princeton Univ. Press, Princeton, NJ.

Rambaut A, Drummond AJ (2003) Tracer. MCMC trace analysis tool version v1.5.0.

Raupach MJ, Thatje S, Dambach J *et al.* (2010) Genetic homogeneity and circum-Antarctic distribution of two benthic shrimp species of the Southern Ocean, *Chorismus antarcticus* and *Nematocarcinus lanceopes*. *Marine Biology*, **157**, 1783–1797.

Rogers AD (2007) Evolution and biodiversity of Antarctic organisms: a molecular perspective. *Philosophical Transactions of the Royal Society of London. Series B, Biological Sciences*, **1488**, 2191–2214.

Rogers AR, Harpending H (1992) Population growth makes waves in the distribution of pairwise genetic differences. *Molecular Biology and Evolution*, **9**, 552–569.

Scherer RP, Aldahan A, Tulaczyk S *et al.* (1998) Pleistocene Collapse of the West Antarctic Ice sheet. *Science*, **281**, 82–85.

Schneider S, Excoffier L (1999) Estimation of demographic parameters from the distribution of pairwise differences when the mutation rates vary among sites: application to human mitochondrial DNA. *Genetics*, **152**, 1079–1089.

Shaw PW, Arkhipkin AI, Al-Khairulla H (2004) Genetic structuring of Patagonian toothfish populations in the Southwest Atlantic Ocean: the effect of the Antarctic Polar Front and deep-water troughs as barriers to genetic exchange. *Molecular Ecology*, **13**, 3293–3303.

Sokolov S, Rintoul SR (2007) On the relationship between fronts of the Antarctic Circumpolar Current and surface chlorophyll concentrations in the Southern Ocean. *Journal of Geophysical Research*, **112**, C07030.

Stamatakis A (2006) RAxML-VI-HPC: maximum likelihood based phylogenetic analyses with thousands of taxa and mixed models. *Bioinformatics*, **22**, 2688–2690.

Strugnell J, Rogers AD, Prodöhl PA *et al.* (2008) The thermohaline expressway: the Southern Ocean as a centre of origin for deep-sea octopuses. *Cladistics*, **24**, 1–8.

Strugnell JM, Allcock AL, Watts PC (2009) A panel of microsatellite loci from two species of octopus, *Pareledone turqueti* (Joubin, 1905) and *Pareledone charcoti* (Joubin, 1902). *Molecular Ecology Resources*, **9**, 1239–1242.

Sullivan J, Swofford DL, Naylor GJP (1999) The effect of taxon sampling on estimating rate heterogeneity parameters of maximum-likelihood models. *Molecular Biology and Evolution*, **16**, 1347–1356.

Thatje S, Hillenbrand C-D, Larter R (2005) On the origin of Antarctic marine benthic community structure. *Trends in Ecology and Evolution*, **20**, 534–540.

Thornhill DJ, Mahon AR, Norenburg J *et al.* (2008) Open-ocean barriers to dispersal: a test case with the Antarctic Polar Front and the ribbon worm *Parborlasia corrugatus* (Nemertea:Lineidae). *Molecular Ecology*, **17**, 5104–5117.

Wilson AC, Cann RL, Carr SM *et al.* (1985) Mitochondrial DNA and two perspectives on evolutionary genetics. *Biological Journal of the Linnean Society*, **26**, 375–400.

Wilson NG, Schrödl M, Halanych KM (2009) Ocean barriers and glaciation: evidence for explosive radiation of mitochondrial lineages in the Antarctic sea slug *Doris kerguelenensis* (Mollusca, Nudibranchia). *Molecular Ecology*, **18**, 965–984.

Yang Z (1993) Maximum-likelihood estimation of phylogeny from DNA sequences when substitution rates differ over sites. *Molecular Biology and Evolution*, **10**, 1396–1401.

J.M.S's research interests include the molecular evolution of molluscs, evolution in Antarctic and deep sea taxa and the application of next-generation sequencing technologies to fisheries and aquaculture. P.C.W. is a molecular ecologist who seeks to identify the processes that determine the scale and extent of population divergence and adaptation. P.S. is interested in the development and application of genetic techniques in order to help understand evolutionary processes. A.L.A. is interested in the evolution and ecology of cephalopods and other molluscs, particularly the groups that have radiated in the Southern Ocean and the deep sea.

Data accessibility

DNA sequences (including sampling data): Genbank accessions JN242814–JN243099, BOLD project folder ''PARAL Pareledone turqueti''.

Microsatellite data: DRYAD entry doi: 10.5061/dryad.4350cp14.

Supporting information

Additional supporting information may be found in the online version of this article.

Table S1 Probability of deviating from expected Hardy–Weinberg equilibrium (HWE) conditions for large samples of the Antarctic benthic octopus *P. turqueti*.

Table S2 Estimates of genetic differentiation (F_{ST}) at microsatellite loci for pairs of large samples of the Antarctic octopus *P. turqueti*.

Table S3 Average proportions of membership (Q) of samples of the Antarctic octopus *P. turqueti* to one of three or six hypothetical model clusters identified by Structure (see Fig. S2); clusters contributing most to each geographic location are highlighted bold.

Fig. S1 Graphical detection of the most likely number of distinct model clusters (K) in a genetic sample using Structure (Pritchard *et al*. 2003) software.

Fig. S2 Probabilities of individual membership to cluster in either (a) a three or (b) six cluster simulation using Structure (Pritchard *et al.* 2003) based on microsatellite genotype frequencies of *P. turqueti* from the Southern Ocean.

Fig. S3 Variation in the level of genetic differentiation [$F_{ST}/(1 - F_{ST})$] with geographic distance (log km) between pairs of samples of the Antarctic octopus *P. turqueti* ($r = 0.14$, $n = 28$, $P = 0.33$, Mantel test).

Fig. S4 Mismatch distributions based on MT-CO1 haplotypes for nine different geographical partitions of the benthic octopus *P. turqueti* from locations around Antarctica (for full details see Results and also Table 2 in the main body text).

Fig. S5 Bayesian skyline plots based on MT-CO1 haplotypes for nine different geographical partitions of the benthic octopus *P. turqueti* from locations around Antarctica (for full details see Results and Table 2 in the main body text).

Please note: Wiley-Blackwell are not responsible for the content or functionality of any supporting information supplied by the authors. Any queries (other than missing material) should be directed to the corresponding author for the article.